ORIGINAL RESEARCH

Modified murine intracranial aneurysm model: aneurysm formation and rupture by elastase and hypertension

Koji Hosaka, Daniel P Downes, Kamil W Nowicki, Brian L Hoh

Department of Neurosurgery, University of Florida, Gainesville, Florida, USA

Correspondence to
Dr Koji Hosaka, Department of Neurosurgery, University of Florida, P O Box 100265, Gainesville, FL 32610, USA; koji@ufl.edu

Received 30 April 2013
Revised 16 July 2013
Accepted 22 July 2013
Published Online First 13 August 2013

To cite: Hosaka K, Downes DP, Nowicki KW, *et al*. *J NeuroIntervent Surg* 2014;**6**:474–479.

ABSTRACT

Introduction Cerebral aneurysms occur in up to 5% of the population. There are several murine models of aneurysms; however, all have limitations and none reproducibly model aneurysm rupture. To fulfill this need, we modified two current rodent aneurysm models to create a murine model which reproducibly produces intracranial aneurysms and rupture.

Methods The left common carotid arteries and the right renal arteries were ligated in C57BL/6 female mice with a hypertensive diet. One week later, small burr holes were created with a stereotactic frame using the following stereotactic measurements: 1.2 mm rostral and 0.7 mm lateral to the right of the bregma. A 26 G needle was gradually advanced via the burr hole until contact with the skull base, upon which the needle was pulled back 0.3 mm. Five, 10 and 20 μL of 10 U/mL elastase solution and 10 μL of 1 U/mL elastase solution were stereotactically injected into the basal cisterns. Angiotensin II was then continually infused at a dose of 1000 ng/kg/min via an osmotic pump placed subcutaneously. In the control mice, 20 μL bromophenol blue solution was injected. Three weeks later, or earlier if mice expired prior to 3 weeks, the circle of Willis was inspected by microscopy for aneurysm formation and/or signs of rupture. Histological analyses were then performed to evaluate elastic lamina destruction, inflammatory cell and macrophage infiltration, absence of intimal endothelial cells and thickening of the smooth muscle layer within the aneurysm wall. To compare with human aneurysms, human aneurysm specimens (n=35; 34 unruptured and 1 ruptured) and normal control superficial temporal arteries (STAs) (n=9) were examined.

Results All mice given 5, 10 and 20 μL of 10 U/mL elastase solution developed intracranial aneurysms within the circle of Willis; 40%, 60% and 50% of mice had ruptured aneurysms, respectively. In mice given 10 μL of 1.0 U/mL elastase solution, 90% developed intracranial aneurysms and 20% had ruptured aneurysms. Aneurysms were confirmed by examining the destruction of the elastic lamina. Aneurysms consistently demonstrated CD45 positive inflammatory cell and F4/80 positive macrophage infiltration within the aneurysm wall which was not present in the circle of Willis of normal sham-operated mice. These results were similar to those in human aneurysms and STA control arteries.

Conclusions We modified two current rodent aneurysm models to create a murine model that produces consistent aneurysms and rupture and can be used for studying cerebral aneurysm formation, rupture and treatment.

INTRODUCTION

Cerebral aneurysms (CA) occur in up to 5% of the population.[1 2] Subarachnoid hemorrhage (SAH) caused by CA rupture occurs in approximately 30 000 individuals in the USA each year and comprises up to 7% of all strokes.[3] Approximately half of all patients with SAH die and, of the surviving patients, half have complications which interfere with daily life.[4] Little is known about the pathophysiology of CA formation. Inflammatory cells such as macrophages have been found in the walls of human CAs,[5–8] but it is not known whether inflammation causes aneurysm formation or whether it is an epiphenomenon to aneurysm formation. To develop novel treatments for aneurysms, a better understanding of the mechanism of aneurysm formation is necessary.

A number of animal aneurysm models including saccular and fusiform aneurysms have been described.[9–19] These aneurysm models are used in both larger animals (dogs, pigs and rabbits) and smaller animals (rodents). Among the aneurysm models available, however, there are only a few intracranial saccular aneurysm models and all have limitations.

Morimoto *et al* described a murine CA model in which approximately 78% of mice develop aneurysms at the anterior cerebral artery (ACA) and olfactory artery (OA) bifurcation. A limitation of this model, however, is that aneurysm development requires >4 months. Also, while some of the aneurysms can be observed under light microscopy, other aneurysms are so small that electron microscopy is needed to evaluate for aneurysms. Hashimoto *et al* described an elastase-induced aneurysm model in hypertensive mice, but this model is not intended for studying aneurysm rupture.

We modified these two current models and developed a murine model to study aneurysm formation and rupture.

METHODS

Animals

All animal procedures were performed under the approval of the University of Florida Animal Care and Use Committee.

Human aneurysm specimens

The collection and studies of human aneurysm specimens and superficial temporal arteries (STAs) were performed under approval of our Institutional Review Board (IRB). Patients signed informed IRB

research consent before undergoing aneurysm surgery. Aneurysm (n=35; 34 unruptured and 1 ruptured) and control STA specimens (n=9) were harvested at the time of craniotomy and aneurysm clipping surgery. Aneurysm specimens were collected from the aneurysm dome. The tissues were immediately transferred into 4% paraformaldehyde.

Description of model

Female C57BL/6 mice (Charles River, Wilmington, Massachusetts, USA) aged 7–10 weeks were used. To induce chronic hypertension, the right renal artery and the left common carotid artery (LCCA) were ligated using 8–0 nylon suture (Ethicon, Somerville, New Jersey, USA). One week later the mice were fixed in the stereotaxic frame with a mouse adaptor (Stoelting, Wood Dale, Illinois, USA). A small right burr hole was made with a drill using coordinates obtained from the Mouse Brain Atlas (the Mouse Brain in Stereotaxic Coordinates, 2nd edition): 1.2 mm rostral and 0.7 mm lateral of the bregma. A Hamilton syringe with a 26G needle (Hamilton, Reno, Nevada, USA) adjoined to a syringe pump (Cole-Parmer, Vernon Hills, Illinois, USA) was advanced until contact with the skull base, upon which the needle was pulled back 0.3 mm. Elastase solution (Worthington Biochemical Corporation, Lake Wood, New Jersey, USA) was then injected into the right basal cistern. After elastase injection and closure of the skin over the burr hole, a separate small incision was made in the dorsal skin between the scapulae. A micro-osmotic pump (Durect, Cupertino, Massachusetts, USA) containing angiotensin II (BACHEM, Torrance, California, USA) in phosphate-buffered saline (PBS; 1000 ng/kg/min) was implanted into a subcutaneous pocket. The mice were fed a hypertensive diet (8% sodium chloride and 0.12% β-aminopropionitrile; Sigma-Aldrich, St Louis, Missouri, USA).

The animals were closely monitored each day for any neurological symptoms until the end of the study. If any neurological symptoms such as inactivity, circling paresis or ≥15% weight loss were observed, the animal was immediately killed and the circle of Willis inspected.

Three weeks after the elastase injection the mice were killed by cardiac perfusion of 3 mL 4% paraformaldehyde (PFA; Sigma-Aldrich) through the left ventricle. Immediately after the PFA cardiac perfusion, bromophenol blue dissolved in 10% (w/v) gelatin/PBS solution was perfused through the left ventricle. The brains were harvested carefully followed by inspection of the circle of Willis by light microscopy.

Bromopenol blue dye injection study

To test the coordinates for injection and volume of solution necessary for aneurysm formation, female C57BL/6 mice (Charles River) aged 7–10 weeks were used. The coordinates were obtained from either the Mouse Brain Atlas (1.2 mm rostral and 0.7 mm lateral of bregma or 1.2 mm rostral and 1.0 mm lateral of bregma) or a previous model.[18] The total volume of 5, 10 or 20 μL of bromophenol blue solution (Sigma-Aldrich) (N=10 mice per cohort) was injected at the rate of 2 μL/min. Mice were immediately killed by cardiac perfusion from the left ventricle using 3 mL 4% PFA. The brains of the mice were dissected to determine the success of different injections.

Elastase dose study

In mice in which the aneurysm model was performed, a total volume of 5, 10 or 20 μL elastase solution (10 units/mL in PBS), 10 μL elastase solution (1.0 unit/mL in PBS) or 20 μL bromophenol blue (n=10 mice for each) was injected into the right basal cistern at a rate of 2 μL/min via a stereotactic needle.

Histological analysis

After 24 h of paraformaldehyde fixation, specimens were either frozen prepared or paraffin embedded. For cryosection, the mouse tissues were transferred into 18% sucrose solution in PBS for 24 h at 4°C and embedded in OCT compound. The blocks were then sectioned into 5 μm using a cryostat. For paraffin embedding, the human tissues were transferred into 70% ethyl alcohol followed by embedding using a Milestone Histos 5 Microwave Histoprocessor. The blocks were sectioned using a microtome into 5 μm sections. To evaluate the elastic lamina in mouse and human specimens, elastic Van Gieson staining was performed using an elastic stain kit (Thermo Scientific, Waltham, Massachusetts, USA) as indicated by the manufacturer. Immunohistochemistry (IHC) was performed on mouse and human aneurysms and control specimens. To evaluate aneurysm formation, the following antibodies were used for IHC: anti-mouse CD45 (Abcam, Cambridge, Massachusetts, USA), anti-human CD45 (DAKO, Carpinteria, California, USA), anti-mouse F4/80 (AbD Serotec, Raleigh, North Carolina, USA), anti-CD68 (Abcam), anti-MECA32 (BD Pharmingen, San Jose, California, USA), anti-human vWF (BD Pharmingen) and anti-α-smooth muscle actin (SMA) (Sigma). Antigen heat retrieval with Citra buffer (pH 6.0) was required for F4/80, CD68 and vWF staining. DAKO target retrieval solution was used for CD45 and MECA32 staining.

Fluorescent and light microscopy

Mouse aneurysms were tested and imaged using Leica dissection microscope with Volocity 3D analysis software and imaged using Olympus IX71 inverted fluorescent scope (Olympus, Center Valley, Pennsylvania, USA) with Image Pro software.

RESULTS

Validation of stereotactic coordinates (bromophenol blue solution injection into right basal cistern)

In mice that received 5, 10 or 20 μL bromophenol blue solution into the right basal cistern using our stereotactic coordinates (1.2 mm rostral and 0.7 mm lateral of bregma), blue dye was seen within the circle of Willis in all brains (10 of 10 each; figure 1A). In mice that received bromophenol blue injected using other coordinates (1.2 mm rostral and 1.0 mm lateral of bregma or previously described coordinates[18]), only 30% (3 of 10) and 50% (5 of 10) mice were found to have blue dye at the circle of Willis, respectively (figure 1B).

Elastase dose study

All mice that received 5, 10 or 20 μL of 10 U/mL elastase solution and 90% of mice that received 10 μL of 1.0 U/mL elastase solution were found to have circle of Willis aneurysms (figure 2A). Aneurysm rupture occurred in 20% of mice that received 10 μL of 1.0 U/mL elastase, in 40% that received 5 μL of 10 U/mL elastase solution, 60% that received 10 μL of 10 U/mL elastase solution and in 50% that received 20 μL of 10 U/mL elastase solution (figure 2A). A small hemorrhage was observed in one of the mice that received 10 μL of 1.0 U/mL elastase solution and no aneurysm formation or neurological symptoms were observed. Neurological symptoms were observed within 14 days in 40% of mice that received 5 μL of 10 U/mL elastase solution, in 50% that received 10 μL of 10 U/mL elastase solution, in 50% that received 20 μL of 10 U/mL elastase solution and in none of the mice that received 10 μL of 1.0 U/mL elastase solution, which is significantly lower ($p<0.05$) than both the 10 μL of 10 U/mL dose and the

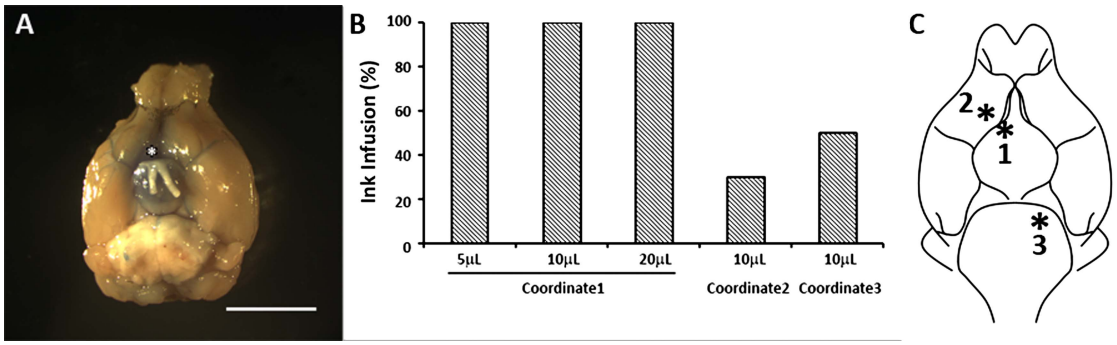

Figure 1 Infusion of bromophenol blue at different coordinates. (A) Light microscopic image of bromophenol blue infusion in the right basal cistern. After injection of bromophenol blue using coordinate 1 (1.2 mm rostral and 0.7 mm lateral of bregma), blue dye was seen within the circle of Willis (COW) in all brains (10 of 10 each). Asterisk indicates the site of injection (scale bar=5 mm). (B) Success rates of bromophenol blue dye infusion within the COW using various stereotactic coordinates. (C) Image of murine COW with coordinates (coordinate 1: 1.2 mm rostral and 0.7 mm lateral of bregma; coordinate 2: 1.2 mm rostral and 1.0 mm lateral of bregma; coordinate 3:−2.5 mm rostral and 1.0 mm lateral of bregma, 5.0 mm ventral to the skull surface).

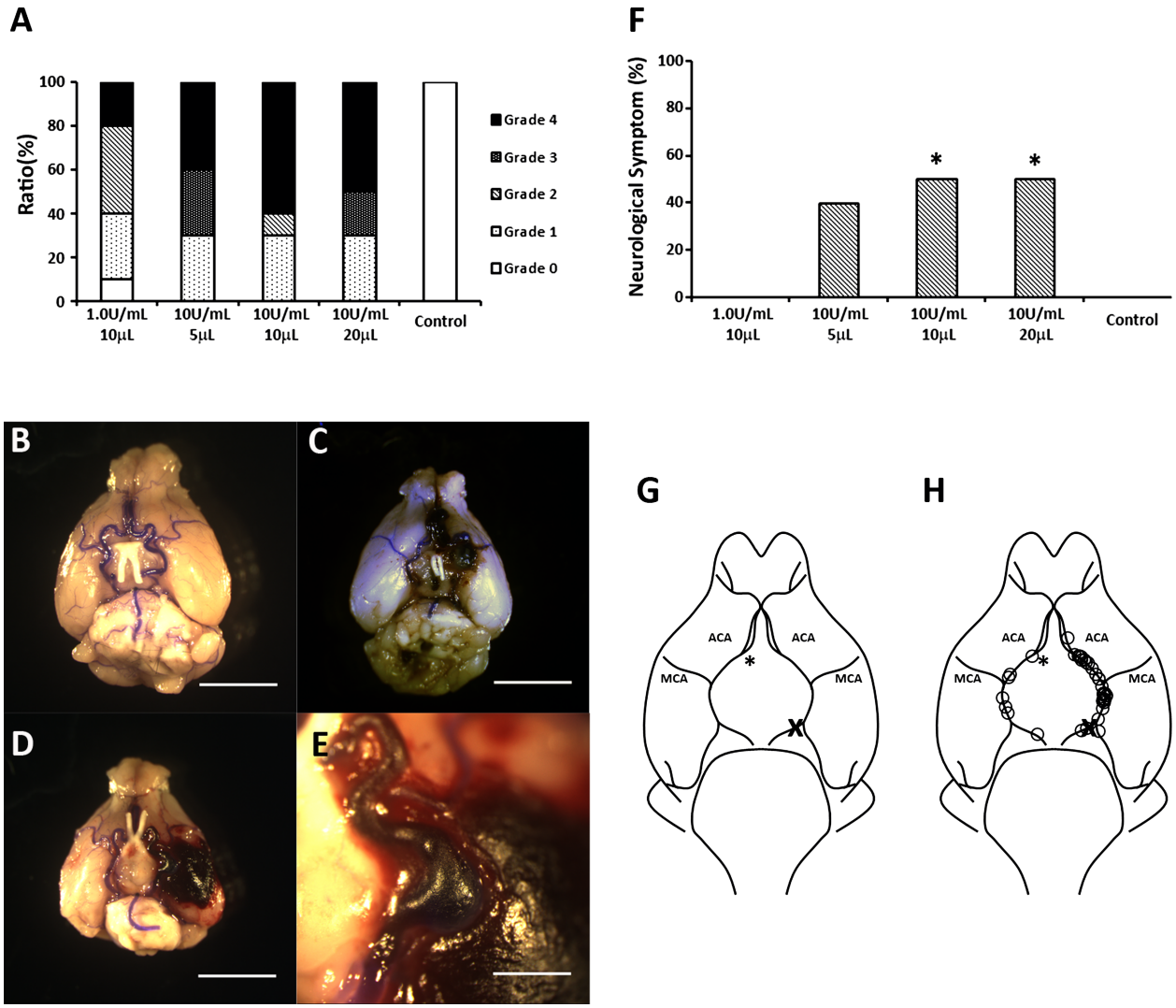

Figure 2 Dose-dependent effects of elastase injection on intracranial aneurysm formation. (A) Comparison between the concentration and volume of elastase solution and aneurysm formation within the circle of Willis (COW). Grade 0: normal arteries; Grade 1: abnormal/aneurysmal arteries; Grade 2: one aneurysm within the COW; Grade 3: two or more aneurysms within the COW; Grade 4: ruptured aneurysm. Light microscopic images indicate a Grade 1 (B), Grade 3 (C) and Grade 4 (D) aneurysm (scale bar=5 mm) and a magnified image of a ruptured aneurysm (scale bar=1 mm) (E). (F) Ratio of mice that showed neurological symptoms within 14 days after elastase injection (*p<0.05). (G) Image of murine COW. (H) Locations of aneurysm found within the COW. Most of the aneurysms (84.1%) were formed at the left side of the COW. Asterisk indicates the site of injection. X indicates the site of ligation of common carotid artery.

20 μL of 10 U/mL dose (figure 2F). None of the mice that received 20 μL bromophenol blue solution had aneurysm rupture or hemorrhage. Thirty-seven of 44 aneurysms (84.1%) were formed at the left side of the circle of Willis, which was the same side as the common carotid artery ligations (figure 2G).

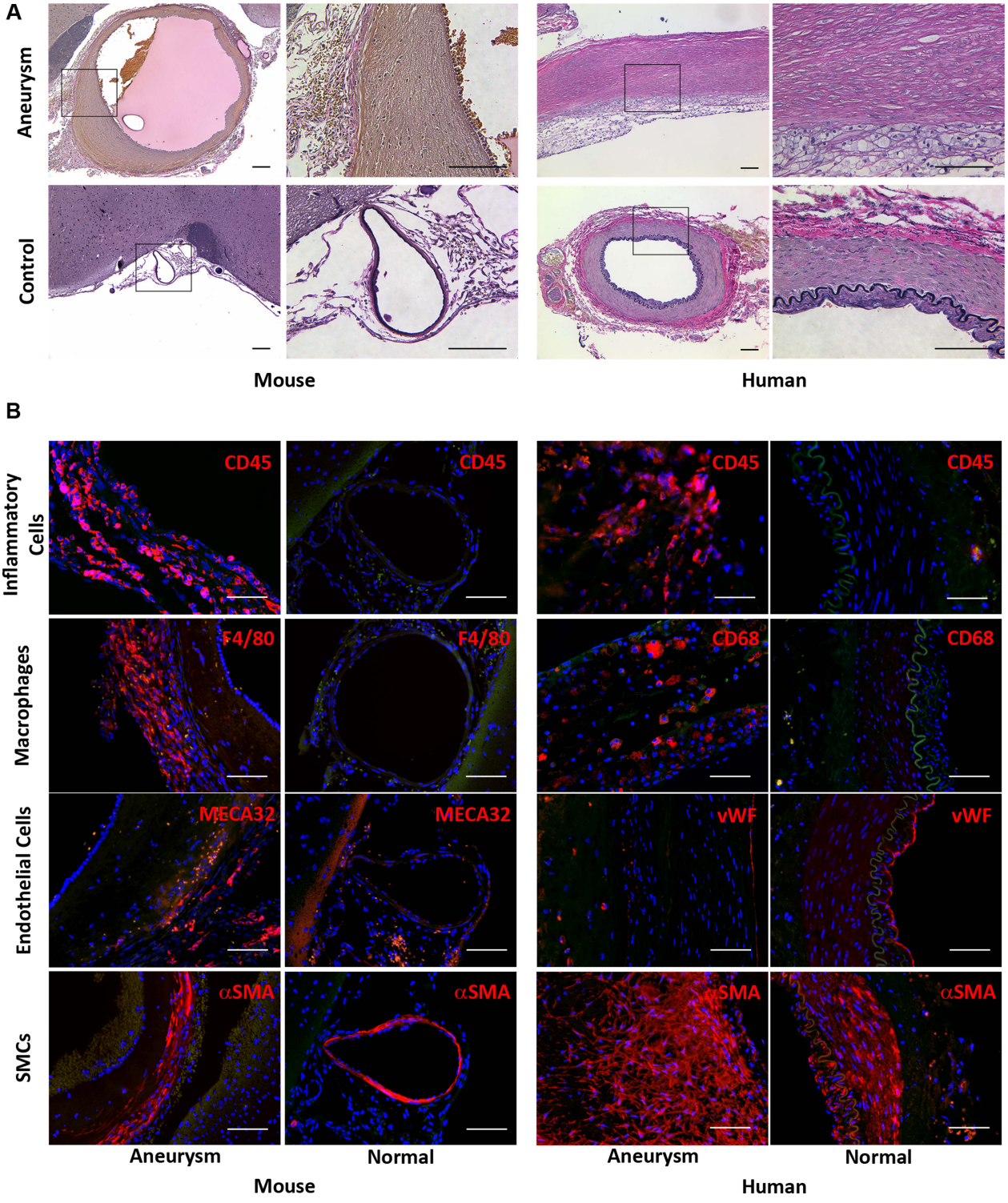

Figure 3 Histological analysis of murine and human intracranial aneurysms. (A) Representative light microscopic images of murine and human intracranial aneurysm and control artery with elastic Van Gieson staining. The staining revealed destruction of elastic lamina in both murine and human aneurysms. Elastic fibers: dark blue to black; nuclei: black; collagen: red; other structures: yellow (scale bar=100 μm). (B). Fluorescent microscopic images showing infiltration of inflammatory (CD45 (red) positive) cells and macrophages (F4/80 (red) positive cells) into the murine aneurysm but the absence of both in the control artery. Destruction of intimal endothelial (MECA32 (red) positive) cells and thickening of the smooth muscle (αSMA (red) positive) cell layer were observed within the murine aneurysm wall. Similar results were observed in human aneurysm specimens. Blue: 4′,6-diamidino-2-phenylindole (scale bar=100 μm).

Histological evaluation of aneurysm

Histological analysis by elastic Van Gieson staining of the circle of Willis of mice that developed aneurysms demonstrated destruction of the elastic lamina within the aneurysm wall (figure 3A). IHC analysis of murine aneurysms revealed inflammatory cell (CD45 positive cells) and especially macrophage (F4/80 positive cells) infiltration in the aneurysm wall, whereas none were found in the circle of Willis of sham-operated mice (figure 3B). Partial or complete absence of intimal endothelial cells, capillary formation (MECA32 positive cells) and thickening of the smooth muscle cell layer in murine aneurysms were observed. These results are similar to those found in human aneurysms (figure 3B).

DISCUSSION

Little is known about the pathophysiology of CA formation and rupture. While studies of human aneurysm specimens collected during surgery[6 20–22] are instrumental to our basic understanding of CAs, they are limited in that these tissues are, in most cases, in the final stage of aneurysm growth. It is difficult to elucidate the role of cytokines and inflammation in earlier stages of aneurysm growth and development because human samples are generally not available at these early stages. A reliable animal model is necessary to study aneurysm pathophysiology and to identify potential novel therapeutic targets.

In Morimoto's established rodent model of CA, approximately 78% of animals develop aneurysms within the circle of Willis at the site of ACA and OA bifurcation.[17] However, one of the limitations of this model is that aneurysm development takes >4 months. Another limitation is the small size of the aneurysms, some of which are so small that they require visualization with an electron microscope. Hashimoto *et al* described an elastase-induced hypertensive mouse aneurysm model which has a much shorter time period of aneurysm development. Aneurysms occur in approximately 77% of wild type mice.[18] In our experience, the incidence of aneurysm formation with this model is inconsistent. One explanation may be the stereotactic coordinates described in the model paper,[18] which we tested with bromophenol blue dye injection and found that the dye surrounded the circle of Willis in only 50% of mice (figure 1B).

In our modified murine intracranial aneurysm model, mice consistently develop aneurysms. Inflammatory cells and macrophages are routinely found within the aneurusmal wall and not in the normal circle of Willis. To our knowledge, our model is the first to consistently produce aneurysm rupture in an elastase dose-dependent manner. This is critical because further investigations should study the pathophysiology of aneurysm formation and also the mechanisms by which aneurysms rupture, since there are limitations in using human specimens. One of the limitations in using human aneurysm specimens is that many cell responses/pathways occur during the earlier stages of aneurysm formation and development but, in many cases, aneurysm specimens are surgically removed in the later stages of aneurysm development. Particularly for ruptured aneurysm studies in human specimens, it is difficult to confirm whether or not all the inflammatory responses observed in the tissues are related to aneurysm development/rupture. Based on our elastase dose study, we recommend using 10 µL of 1.0 U/mL elastase to study aneurysm formation without rupture and 10 µL of 10 U/mL elastase to study aneurysm rupture.

Hemodynamic stress is known to be a key factor in the pathophysiology of intracranial aneurysm formation.[23–26] We observed more aneurysm formation on the left side of the circle of Willis (figure 2C), since the hemodynamics had been changed by ligation of the LCCA. This model can be a useful tool for investigating the correlation between stress changes and formation of aneurysms.

A limitation of this model is that aneurysm formation by elastase injection may not be the same as non-enzyme/chemical-induced aneurysms. The process of naturally occurring CAs is not known. We have found that elastase is necessary to produce the consistency of aneurysm formation in this model and other elastase aneurysm models.[18]

CONCLUSION

We describe a modified murine intracranial aneurysm model that produces consistent aneurysms, demonstrates inflammatory cell infiltration in the aneurysm wall and produces aneurysm rupture in a dose-dependent manner.

Contributors KH contributed to the conception and design, analysis and interpretation of data, drafting the article and final approval of the version to be published. DPD and KWN contributed to the analysis and interpretation of data, revising the article critically for important intellectual content and final approval of the version to be published. BLH contributed to the conception and design, revising the article critically for important intellectual content and final approval of the version to be published.

Funding This work was supported by NIH grant number K08 NS067058-01, Thomas H. Maren Foundation and Brain Aneurysm Foundation. to BLH.

Competing interests None.

Ethics approval Ethical approval was obtained from University of Florida Institutional Review Board and Institutional Animal Care and Use Committee.

Provenance and peer review Not commissioned; externally peer reviewed.

REFERENCES

1 Wiebers DO, Whisnant JP, Huston J III,, *et al* Unruptured intracranial aneurysms: natural history, clinical outcome, and risks of surgical and endovascular treatment. *Lancet* 2003;362:103–10.
2 Brisman JL, Song JK, Newell DW. Cerebral aneurysms. *N Engl J Med* 2006;355:928–39.
3 Feigin VL, Lawes CM, Bennett DA, *et al*. Stroke epidemiology: a review of population-based studies of incidence, prevalence, and case-fatality in the late 20th century. *Lancet Neurol* 2003;2:43–53.
4 van Gijn J, Kerr RS, Rinkel GJ. Subarachnoid haemorrhage. *Lancet* 2007;369:306–18.
5 Chyatte D, Bruno G, Desai S, *et al*. Inflammation and intracranial aneurysms. *Neurosurgery* 1999;45:1137–46.
6 Kataoka K, Taneda M, Asai T, *et al*. Structural fragility and inflammatory response of ruptured cerebral aneurysms. A comparative study between ruptured and unruptured cerebral aneurysms. *Stroke* 1999;30:1396–401.
7 Frosen J, Piippo A, Paetau A, *et al*. Remodeling of saccular cerebral artery aneurysm wall is associated with rupture: histological analysis of 24 unruptured and 42 ruptured cases. *Stroke* 2004;35:2287–93.
8 Kosierkiewicz TA, Factor SM, Dickson DW. Immunocytochemical studies of atherosclerotic lesions of cerebral berry aneurysms. *J Neuropathol Exp Neurol* 1994;53:399–406.
9 Anon . Mastectomy or conservation: the patient's choice. *BMJ* 1989;298:49.
10 Altes TA, Cloft HJ, Short JG, *et al*. 1999 ARRS Executive Council Award. Creation of saccular aneurysms in the rabbit: a model suitable for testing endovascular devices. American Roentgen Ray Society. *AJR Am J Roentgenol* 2000;174:349–54.
11 Bavinzski G, al-Schameri A, Killer M, *et al*. Experimental bifurcation aneurysm: a model for in vivo evaluation of endovascular techniques. *Minim Invasive Neurosurg* 1998;41:129–32.
12 Graves VB, Ahuja A, Strother CM, *et al*. Canine model of terminal arterial aneurysm. *AJNR Am J Neuroradiol* 1993;14:801–3.
13 Guglielmi G, Ji C, Massoud TF, *et al*. Experimental saccular aneurysms. II. A new model in swine. *Neuroradiology* 1994;36:547–50.
14 Hoh BL, Rabinov JD, Pryor JC, *et al*. A modified technique for using elastase to create saccular aneurysms in animals that histologically and hemodynamically resemble aneurysms in human. *Acta Neurochir (Wien)* 2004;146:705–11.

15 Hoh BL, Velat GJ, Wilmer EN, *et al*. A novel murine elastase saccular aneurysm model for studying bone marrow progenitor-derived cell-mediated processes in aneurysm formation. *Neurosurgery* 2010;66:544–50.
16 Miskolczi L, Guterman LR, Flaherty JD, *et al*. Saccular aneurysm induction by elastase digestion of the arterial wall: a new animal model. *Neurosurgery* 1998;43:595–600.
17 Morimoto M, Miyamoto S, Mizoguchi A, *et al*. Mouse model of cerebral aneurysm: experimental induction by renal hypertension and local hemodynamic changes. *Stroke* 2002;33:1911–15.
18 Nuki Y, Tsou TL, Kurihara C, *et al*. Elastase-induced intracranial aneurysms in hypertensive mice. *Hypertension* 2009;54:1337–44.
19 Spetzger U, Reul J, Weis J, *et al*. Microsurgically produced bifurcation aneurysms in a rabbit model for endovascular coil embolization. *J Neurosurg* 1996;85:488–95.
20 Hasan D, Chalouhi N, Jabbour P, *et al*. Macrophage imbalance (M1 vs. M2) and upregulation of mast cells in wall of ruptured human cerebral aneurysms: preliminary results. *J Neuroinflammation* 2012;9:222.
21 Kilic T, Sohrabifar M, Kurtkaya O, *et al*. Expression of structural proteins and angiogenic factors in normal arterial and unruptured and ruptured aneurysm walls. *Neurosurgery* 2005;57:997–1007.
22 Wei H, Mao Q, Liu L, *et al*. Changes and function of circulating endothelial progenitor cells in patients with cerebral aneurysm. *J Neurosci Res* 2011;89:1822–8.
23 Aoki T, Nishimura M, Matsuoka T, *et al*. PGE(2)-EP(2) signalling in endothelium is activated by haemodynamic stress and induces cerebral aneurysm through an amplifying loop via NF-kappaB. *Br J Pharmacol* 2011;163:1237–49.
24 Kadirvel R, Ding YH, Dai D, *et al*. The influence of hemodynamic forces on biomarkers in the walls of elastase-induced aneurysms in rabbits. *Neuroradiology* 2007;49:1041–53.
25 Sakamoto N, Saito N, Han X, *et al*. Effect of spatial gradient in fluid shear stress on morphological changes in endothelial cells in response to flow. *Biochem Biophys Res Commun* 2010;395:264–9.
26 Szymanski MP, Metaxa E, Meng H, *et al*. Endothelial cell layer subjected to impinging flow mimicking the apex of an arterial bifurcation. *Ann Biomed Eng* 2008;36:1681–9.